Pressure-induced structural sequence in $ThAl_2$

N. V. Chandra Shekar,* P. Ch. Sahu, Mohammad Yousuf, and K. Govinda Rajan
Advanced Materials Laboratory, Materials Science Division, Indira Gandhi Centre for Atomic Research, Kalpakkam 603 102, Tamil Nadu, India

(Received 14 June 1996; revised manuscript received 26 August 1996)

On the application of pressure at 300 K, $ThAl_2$ (AlB_2-type hexagonal at STP) exhibits an isostructural transition at around 5.5 GPa. Later it undergoes a phase transition from hexagonal to orthorhombic structure at 12 GPa and then to tetragonal at about 25 GPa. This pressure-induced structural sequence is observed rarely for an AlB_2-type f-electron system. Comparison is made to existing structural data. [S0163-1829(96)00946-0]

Pressure-induced structural sequences observed along the homologues offer an excellent means of correlation between the crystal structures and prediction of new structures. Studies on such sequences are now available for many systems. If one considers the f-electron-based compounds, extensive research has focused on the monochalcogenides and monopnictides of the lanthanides and actinides. A recent survey by Benedict and Holzapfel[1] reveals that very little work has been done for actinide intermetallic compounds. Systematic studies are lacking, although discrete measurements on a few compounds are reported. These studies are mainly on compounds showing either heavy fermion or spin-fluctuating behavior. The review lists, for example, only four dialuminides for which structural aspects have been investigated up to limited pressure.

With the aim to study systematically, the pressure-induced structural changes in dialuminides of the actinides and rare-earth elements, high-pressure x-ray diffraction study of UAl_2 was taken up and an experiment was performed up to 50 GPa. A reversible structural transition from $MgCu_2$ (fcc, $Fd3m$) to $MgNi_2$ (hexagonal, $P6_3/mmm$) type was observed at around 10 GPa.[2] Based on this work and on the ambient pressure studies of some f-electron-based pseudobinary compounds,[3] we proposed a pressure-induced structural sequence: $MgCu_2 \rightarrow MgNi_2$ $(MgZn_2) \rightarrow MgCu_2$-type structures in all f-electron-based AB_2-type Laves phase compounds.[2] $ThAl_2$ exists in the hexagonal AlB_2-type structure. In that, Godwal *et al.*[4] reported a structural transition from the hexagonal AlB_2 to the cubic $MgCu_2$-type structure at a very low pressure of ≈ 0.3 GPa. Further, their work was restricted to only 10 GPa. We aimed our investigations in chasing the above structural sequence in $ThAl_2$ at still higher pressures. In this paper, results of our structural investigations up to 30 GPa are discussed at length. Our preliminary investigations up to 20 GPa are published elsewhere.[5]

Thorium dialuminide ($ThAl_2$) was prepared in single phase by a standard arc-melting technique. Stoichiometric quantities of Th (99.98% pure) and Al (99.999% pure) were melted several times in inert environment. The arc-melted ingots were then sealed in evacuated silica tubes and annealed at 1100 K for about a month. The powdered samples were characterized by x-ray diffraction using a high-precision Guinier diffractometer described elsewhere.[6]

High pressure x-ray diffraction (HPXRD) was carried out with a Mao-Bell-type diamond-anvil cell in an angle-dispersive mode using the Guinier geometry. The detailed description of the Guinier diffractometer setup for carrying out high-pressure experiments is published elsewhere.[6] The Huber-Guinier diffractometer is in vertical configuration (in symmetric transmission mode) with a Seeman-Bohlin focusing circle of diameter 114.6 mm. It is in combination with a curved-quartz crystal monochromator and a linear position-sensitive detector of length 50 mm. The incident Mo x ray is obtained from a Rigaku 18 kW rotating anode x-ray generator. This diffractometer system gives an almost truly $K\alpha_1$ molybdenum radiation and reduces the scan time for obtaining a readable HPXRD pattern to as low as 1/2 h, compared to 20 h required in a conventional film method. However, a scan time of about 2 h is required to obtain data with good signal-to-noise ratio. The overall resolution is found to be $\delta d/d \approx 0.01-0.02$. A finely powdered sample mixed with Ag was loaded into the stainless-steel gasket hole, along with a mixture of methanol, ethanol, and water in the ratio of 16:3:1 as the pressure-transmitting fluid. The equation of state (EOS) of Ag was used for pressure calibration.

High-pressure x-ray diffraction experiments on $ThAl_2$ were done up to ≈ 30 GPa and the P-V data up to 12 GPa is shown in Fig. 1. In contradiction to an earlier report,[4] it was found that $ThAl_2$ retained its AlB_2-type structure up to a maximum pressure of 12 GPa, where it undergoes a reversible structural transition. Also, it was observed that an isostructural transition, possibly of electronic origin, occurs at around 5.5 GPa. The experiments were repeated several times especially at lower pressures and the x-ray diffraction patterns were carefully observed for any changes for possible transition. But the reported $AlB_2 \rightarrow MgCu_2$ transition at 0.3 GPa was not observed. The volume change across the isostructural transition is about 2%. Figure 2 shows the variation of the lattice parameters of the hexagonal phase as a function of pressure. The plot clearly shows that a decreases monotonously, whereas c drops rather sharply across the isostructural transition at about 5.5 GPa. The P-V data on $ThAl_2$ was fitted to the Birch-Murnaghan EOS (Ref. 7) to obtain the bulk modulus B_0. The value of B_0 obtained in this study is 71 ± 14 GPa up to 5.5 GPa. When the P-V data from 5.5 to 12 GPa were fitted, the value of B_0 obtained was 108 ± 13 GPa.

Figure 3 shows the HPXRD spectra of $ThAl_2$ for AlB_2

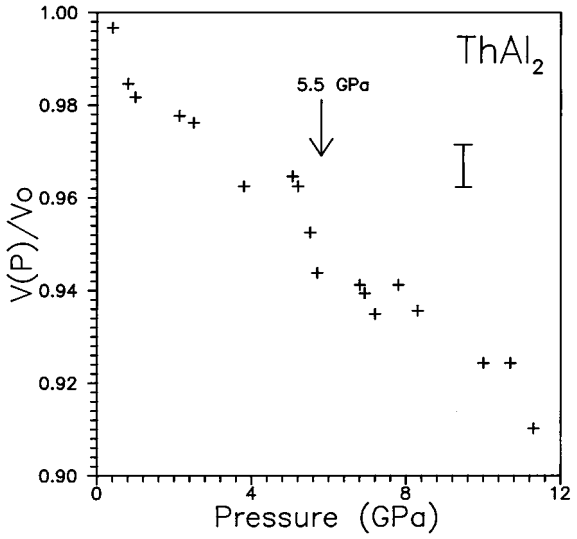

FIG. 1. P-V data of $ThAl_2$ prior to the structural transition. The error bar indicated gives the possible inaccuracies involved in the measurement.

(hexagonal, $Fd3m$) phase at 2.0 GPa, the isostructural phase at 6.0 GPa, and for the high-pressure phases at 18 and 25 GPa, respectively. At around 12 GPa, the x-ray pattern of the high-pressure phase showed the appearance of new peaks and splitting of the parent peaks indicating that the structure must be of lower symmetry. Using the standard trial and error methods, various structures were tried and best fit was obtained for an orthorhombic lattice. All the peaks at 18 GPa could be indexed to the orthorhombic structure with lattice parameters $a=5.25\pm0.01$ Å, $b=11.31\pm0.01$ Å, and $c=4.26\pm0.01$ Å. The orthorhombic phase remained stable up to 22 GPa. Above 22 GPa it was observed that the x-ray diffraction pattern underwent slight changes and featured intensity reversal and reduction in the number of peaks. Remarkable among them was the triple structure around 6° which coalesced to form a single peak. Further high-intensity

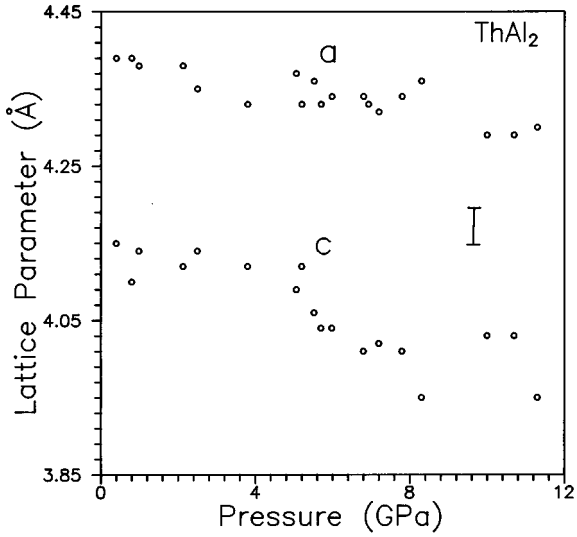

FIG. 2. The lattice parameters a and c of $ThAl_2$ vs pressure prior to the structural transition at about 12 GPa.

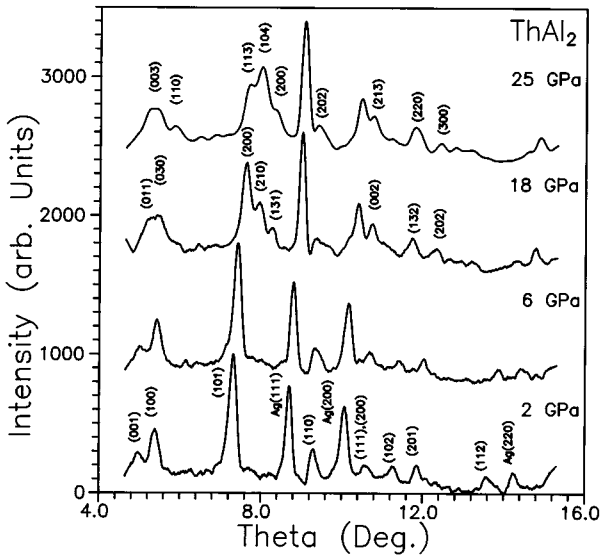

FIG. 3. High-pressure x-ray diffraction spectra of $ThAl_2$ at 2, 6, 18, and 25 GPa. The pattern at 6 GPa clearly shows that there is no change in the structure above the transition at about 5.5 GPa. Pattern at 18 GPa shows orthorhombic phase and that at 25 GPa the tetragonal phase.

triple-peak structure around 8° underwent some reversal in their intensities. This new structure fitted very well to a tetragonal lattice with parameters $a=4.71\pm0.01$ Å and $c=11.28\pm0.05$ Å. Table I lists the calculated and the observed d spacings for the high-pressure phases. Attempts to fit the high-pressure structures to known space groups and structure types were partially successful. The orthorhombic lattice matched very well with $ZrSi_2$-type structure with space-group $Cmcm$ and the tetragonal lattice matched with $ThSi_2$ structure type with space-group $I4_1/amd$. But a peak-to-peak match with proper intensities was not easy, due to the inherent difficulties with the high-pressure x-ray diffraction patterns, namely, (i) poor resolution and (ii) preferred orientation effects leading to arbitrary intensity distribution.

The isostructural transition, in $ThAl_2$ at 5.5 GPa, can be compared with a similar transition in $CeAl_2$ at about 7.7 GPa.[8,9] The volume change across the transition in $CeAl_2$ is around 1% and it has been attributed to the delocalization of the $4f$ electrons. It may be recalled that in pure Ce, the $4f^1$ delocalization pressure is ≈0.7 GPa. However, the situation in $ThAl_2$ is totally different. In Th, the itinerant $5f$ states lie about 1 eV above the Fermi level E_F.[10,11] But due to strong hybridization with the spd states, it manifests itself in several physical properties.[12] The various physical properties and most recently its fcc crystal structure have been attributed to about 4% contribution of $5f$ to the total density of states at E_F.[13] The recent high-pressure experiments by Vohra and co-workers[14] shows an fcc to a bct phase transition at about 70 GPa with the onset of $5f$ occupation at this pressure. This fact has also been confirmed by recent band-structure calculations.[15,16] Preliminary band-structure calculations in $ThAl_2$ using the tight-binding linear muffin-tin orbital method give the position of the $5f$ level about 2.5 eV above the Fermi energy. The isostructural transition in $ThAl_2$ at about 5.5 GPa cannot be correlated with the occupancy of the $5f$ states. However, the increasing effect of the

TABLE I. The calculated and the observed d-spacings with their hkl's for (a) the high-pressure orthorhombic phase at ≈ 18 GPa, with $a = 5.25 \pm 0.01$ Å, $b = 11.31 \pm 0.01$ Å, and $c = 4.26 \pm 0.01$ Å and (b) the high-pressure tetragonal phase at ≈ 25 GPa, with $a = 4.71 \pm 0.01$ Å and $c = 11.28 \pm 0.05$ Å.

(a) Orthorhombic structure				(b) Tetragonal structure			
No.	d_{calc}	d_{obs}	hkl	No.	d_{calc}	d_{obs}	hkl
1	5.65	5.64	020	1	4.35	4.38	101
2	5.25	5.21	100	2	3.76	3.74	003
3	4.26	4.27	001	3	3.33	3.31	110
4	3.98	3.95	011	4	3.19	3.09	111
5	3.77	3.74	030	5	2.87	2.89	112
6	3.40	3.49	021	6	2.49	2.58	113
7	3.30	3.29	101	7	2.42	2.46	104
8	3.17	3.18	111	8	2.35	2.34	200
9	2.85	2.93	121	9	2.25	2.26	005
10	2.82	2.81	031	10	2.17	2.17	202
11	2.62	2.67	200	11	2.07	2.08	211
12	2.55	2.56	210	12	1.97	1.94	212
13	2.48	2.45	131	13	1.83	1.84	213
14	2.26	2.26	050	14	1.80	1.78	204
15	2.19	2.19	211	15	1.66	1.66	220
16	2.13	2.13	002	16	1.59	1.60	222
17	1.99	2.01	051	17	1.57	1.57	300
18	1.94	1.94	112	18	1.51	1.51	302
19	1.88	1.88	060	19	1.47	1.47	206
20	1.85	1.83	032				
21	1.74	1.74	132				
22	1.65	1.65	202				
23	1.59	1.58	251				

$5f$ states on the various physical properties cannot be ruled out. A photoemission study may throw some light on these aspects and also confirms our band-structure calculations.

The motivation in looking for an AlB_2 to $MgCu_2$ structural transition in $ThAl_2$ must have stemmed from an important prediction by Pettifor's two-dimensional (2D) structural map.[17–20] The map predicts that $ThAl_2$ stabilizes in $MgCu_2$-type rather than AlB_2-type structure. The experimental details are not sufficient to speculate as to why such a transition was observed. Recently, Villars, Mathis, and Hullinger[21] have come out with a three-parameter-based structural map that is more practical and has achieved success. If one looks at the prescription for $ThAl_2$, its structure at STP is indeed AlB_2 and not $MgCu_2$, reaffirming our observation. The promise these 3D structural stability maps hold in predicting high-pressure phase transitions has not yet been explored. Pettifor has reviewed in detail the quantum-mechanical basis for the highly successful Miedema macroscopic atom model, used with a great degree of success in predicting structural stability of alloys.[22] It is felt that on similar lines, the quantum-mechanical basis should be sought for Villar's parameters, like the average valence-electron ratio of the constituent atoms, the electronegativity difference, and the pseudopotential radii difference. Once they are defined, then there is a possibility of getting these parameters from band-structure calculations.

Figure 4 shows the structural sequence followed by $ThAl_2$ as a function of pressure. The structural sequence observed in $ThAl_2$ can be rationalized using the available studies on the stability of structures with respect to band filling N of AB_2 structure types.[23,24] The prediction as per the map is hexagonal AlB_2–tetragonal $ThSi_2$–orthorhombic $ZrSi_2$. But in $ThAl_2$ the observed sequence is AlB_2-$ZrSi_2$-$ThSi_2$. The relative stabilities of the $ThSi_2$-type and $ZrSi_2$-type structures have been analyzed by Lee,[23] taking into consideration the two types of networks of bonded atoms, namely, square lattice and zigzag chain, found in these structures. $ThSi_2$ structure seems to be relatively more stable if the interaction between the two types of bonds is strong. In $ThAl_2$, it is noticed that, as a function of pressure, the c axis is affected to a large extent in the beginning, ending with an isostructural transition. Later the a axis begins to change, and a transition to an orthorhombic cell is nucleated. Taking a cue from this evolution, it is possible that in the orthorhombic phase, the distance between the square lattice and the zigzag chain structure is large and the interaction is weak, leading to the $ZrSi_2$-type structure. But as the system is further pressurized, the situation changes and the system acquires sufficient interaction strength to stabilize in the $ThSi_2$-type tetragonal structure.

Turning to our perspective of exploring the possibility of a pressure-induced structural sequence in AB_2 compounds, namely, $MgCu_2 \rightarrow MgNi_2 \rightarrow MgCu_2$, we find that such a sequence is not exhibited by pressure-induced transitions in $ThAl_2$. The reason is that the reported AlB_2 to $MgCu_2$ structural transition,[4] on the basis of which we were motivated to look for the above-structural sequence, was not observed.

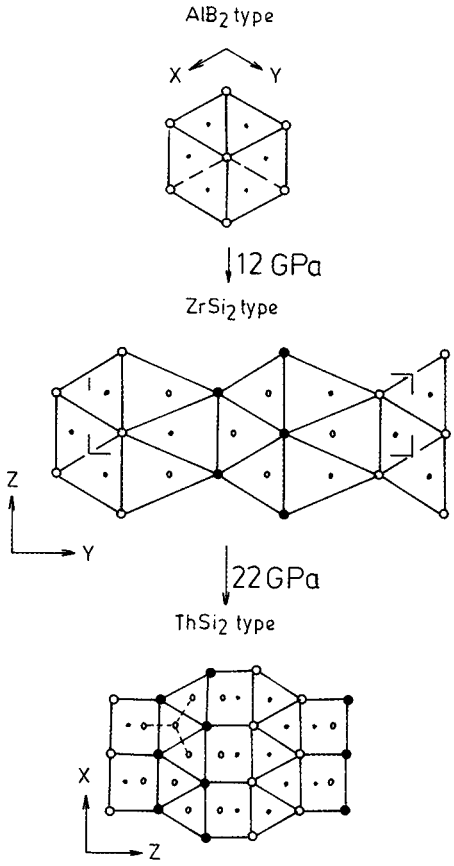

FIG. 4. The structural sequence followed by $ThAl_2$ as a function of pressure. The diagram shows the geometric evolution of various structures $AlB_2(h)$–$ZrSi_2(o)$-$ThSi_2(t)$. The large circles are Al and small circles Th. Open circles are at origin and closed circles at one half perpendicular to the plane of the paper. The AlB_2-type structure is projected on (0001). $ZrSi_2$ is projected on (100) and $ThSi_2$ on (010). $ZrSi_2$ structure type can be regarded as AlB_2 type in which one half of the AlB_2 wall has collapsed and additional Si in tetrahedra between AlB_2-like walls (Al in the case of $ThAl_2$). $ThSi_2$ type of structure is also composed of AlB_2-type walls. But the structure is obtained by a screw operation, namely, translation plus rotation (Ref. 25).

Figure 5 depicts our attempt to systematize the structural data available for AB_2-type intermetallic compounds of lanthanides and actinides. Among the 365 compounds existing in the phase diagram, about 200 compounds stabilize in the

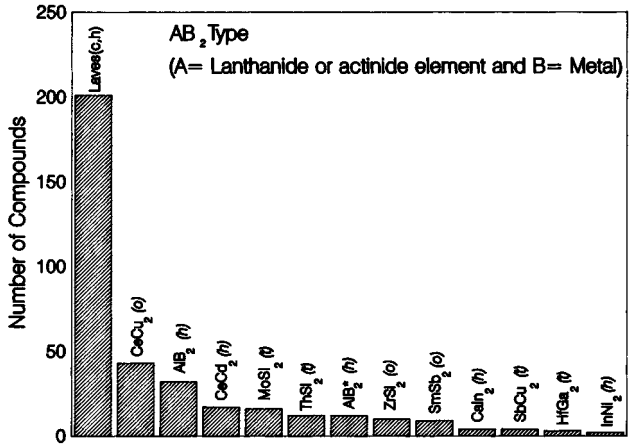

FIG. 5. The bar chart shows the number of compounds adopting different structure types among the AB_2-type lanthanide and actinide intermetallic compounds. (o, orthorhombic; t, tetragonal; h, hexagonal; c cubic.)

cubic $MgCu_2$ Laves phase. This also means that the Laves phase is stable for a wide range of band electrons. This can also be noted from Fig. 5. Is it that once a system is in Laves phase its stability regime under pressure is extended? This is pointed out by structural investigations on many $MgCu_2$-type compounds that stay in this phase even up to fairly high pressures. $LnAl_2$ (Ln=lanthanides) are typical examples that remain in cubic phase under pressure.[26] Our recent high-pressure x-ray diffraction studies on $GdAl_2$ have revealed no structural transitions up to about 30 GPa, the maximum pressure up to which the system was investigated. Incidentally, our investigation on UAl_2 also strengthens this point of view. UAl_2 remains in $MgCu_2$ phase up to about 11 GPa, where it transforms to $MgNi_2$ structure, again a Laves phase. Thereafter, it remains stable in $MgNi_2$ structure up to 50 GPa.[2] It is strongly felt that studies in this direction in the form of high-pressure experiments and calculations on intermetallic compounds exhibiting either AlB_2-type structure or $MgCu_2$-type structure may reveal the structural sequence and the role of the valence electrons in stabilizing these structures.

The authors thank N. Subramanian and M. Sekar for useful discussions and L. M. Sundaram for his help in sample preparation. The authors also thank G. V. N. Rao for his help with the x-ray data analysis software. The authors thank Dr. Kanwar Krishan, Dr. Baldev Raj, and Dr. Placid Rodriguez for their encouragement and support.

*Author to whom correspondence should be addressed. Telex: 041-6244 IGC IN. FAX: 0091(4114)40360.

[1] U. Benedict and W. B. Holzapfel, in *Handbook on the Physics and Chemistry of Rare Earths*, edited by K. A. Gschneidner, Jr., L. Eyring, G. H. Lander, and G. R. Choppin (Elsevier Science, Holland, 1993), p. 245; W. B. Holzapfel, Rep. Prog. Phys. **59**, 29 (1996).

[2] P. Ch. Sahu, N. V. Chandra Shekar, N. Subramanian, Mohammad Yousuf, and K. Govinda Rajan, J. Alloys Compd. **223**, 49 (1995).

[3] A. Slebarski, J. Magn. Magn. Mater. **66**, 107 (1987).

[4] B. K. Godwal, V. Vijaykumar, S. K. Sikka, and R. Chidambaram, Physica **144B**, 44 (1986); J. Phys. F. **16**, 1415 (1986).

[5] N. V. Chandra Shekar, P. Ch. Sahu, M. Sekar, Mohammad Yousuf, and K. Govinda Rajan, Physica B (to be published); N. V. Chandra Shekar, P. Ch. Sahu, M. Sekar, Mohammad Yousuf, and K. Govinda Rajan, Solid State Phys. (India) **38C**, 390 (1995).

[6] P. Ch. Sahu, Mohammad Yousuf, N. V. Chandra Shekar, N. Subramanian, and K. Govinda Rajan, Rev. Sci. Instrum. **66**, 2599 (1995).

[7] F. Birch, Phys. Rev. **71**, 809 (1947); J. Geophys. Res. **57**, 227 (1962).

[8] I. Vedel, A. M. Redon, J. M. Leger, J. M. Magnot, and J. Flouquet, J. Magn. Magn. Mater. **54-57**, 361 (1986).

[9] T. G. Ramesh and W. B. Holzapfel, Pramana **29**, 183 (1987).

[10] J. E. Schirber, F. A. Schmidt, and D. D. Koelling, Phys. Rev. B **16**, 4235 (1977).
[11] H. L. Skriver and J. P. Jan, Phys. Rev. B **21**, 1489 (1979).
[12] J. M. Fournier and R. Troc, in *Handbook on the Physics and Chemistry of Actinides*, edited by A. J. Freeman and G. H. Lander (Elsevier, Amsterdam, 1985), Vol. 2, p. 29.
[13] B. Johansson, R. Ahuja, O. Erikkson, and J. M. Wills, Phys. Rev. Lett. **75**, 280 (1995).
[14] Y. K. Vohra, Physica **B190**, 1 (1993); K. Ghandehari and Y. K. Vohra, Scr. Metall. **27**, 195 (1992).
[15] R. S. Rao, B. K. Godwal, and S. K. Sikka, Phys. Rev. B **46**, 5780 (1992).
[16] O. Eriksson, P. Soderlind, and J. M. Wills, Phys. Rev. B **45**, 12 588 (1992).
[17] D. G. Pettifor, in *Structure Maps, Encyclopedia of Materials Science and Technology*, edited by R. W. Cahn (Pergamon, London, 1988), Suppl. Vol. 1.
[18] D. G. Pettifor, Solid State Commun. **38**, 1219 (1981).
[19] D. G. Pettifor and R. Podloucky, Phys. Rev. Lett. **53**, 1080 (1984); J. Phys. C **19**, 315 (1986).
[20] D. G. Pettifor, New Sci. **110**, 48 (1986).
[21] P. Villars, K. Mathis, and F. Hullinger, in *Cohesion and Structure*, edited by F. R. de Boer and D. G. Pettifor (North-Holland, Amsterdam, 1988), Vol. 2, and references therein.
[22] D. G. Pettifor, in *Solid State Physics*, edited by Henry Ehrenreich and David Turnbull (Academic, New York, 1987), Vol. 40, p. 43.
[23] Stephen Lee, J. Am. Chem. Soc. **113**, 101 (1991).
[24] D. G. Pettifor, in *Materials Science and Technology*, edited by R. W. Cahn, P. Haasen, and E. J. Kramer (VCH, Wiemheim, 1993), Vol. 1, p. 61.
[25] B. G. Hyde and Sten Anderson, *Inorganic Crystal Structures* (Wiley Interscience, New York, 1989).
[26] A. Gleissner, Ph.D. dissertation, Physik-Department, Technische Universitat Munchen, 1992.